

Predicting the Corrosion Rate of Steel in Cathodically Protected Concrete Using Potential Shift

Goyal A, Sadeghi Pouya H, Ganjian E, Olubanwo A, Khorami M
Author post-print (accepted) deposited by Coventry University's Repository

Original citation & hyperlink:

Goyal, A, Sadeghi Pouya, H, Ganjian, E, Olubanwo, A & Khorami, M 2019, 'Predicting the Corrosion Rate of Steel in Cathodically Protected Concrete Using Potential Shift' *Construction and Building Materials*, vol. 194, pp. 344-349.

<https://dx.doi.org/10.1016/j.conbuildmat.2018.10.153>

DOI 10.1016/j.conbuildmat.2018.10.153

ISSN 0950-0618

ESSN 1879-0526

Publisher: Elsevier

NOTICE: this is the author's version of a work that was accepted for publication in *Construction and Building Materials*. Changes resulting from the publishing process, such as peer review, editing, corrections, structural formatting, and other quality control mechanisms may not be reflected in this document. Changes may have been made to this work since it was submitted for publication. A definitive version was subsequently published in *Construction and Building Materials*, [[194,] (2019)] DOI: [10.1016/j.conbuildmat.2018.10.153]

© 2019, Elsevier. Licensed under the Creative Commons Attribution-NonCommercial-NoDerivatives 4.0 International

<http://creativecommons.org/licenses/by-nc-nd/4.0/>

Copyright © and Moral Rights are retained by the author(s) and/ or other copyright owners. A copy can be downloaded for personal non-commercial research or study, without prior permission or charge. This item cannot be reproduced or quoted extensively from without first obtaining permission in writing from the copyright holder(s). The content must not be changed in any way or sold commercially in any format or medium without the formal permission of the copyright holders.

This document is the author's post-print version, incorporating any revisions agreed during the peer-review process. Some differences between the published version and this version may remain and you are advised to consult the published version if you wish to cite from it.

Predicting the Corrosion Rate of Steel in Cathodically Protected Concrete Using Potential Shift

Arpit Goyal*

PhD scholar, Centre for the Build and Natural Environment, Engineering, Environment, & Computing Building, Coventry University,
Coventry, CV1 2JH, United Kingdom, Email: goyala4@uni.coventry.ac.uk

Homayoon Sadeghi Pouya

Research Fellow, Centre for the Build and Natural Environment, Engineering, Environment, & Computing Building, Coventry University,
Coventry, CV1 2JH, United Kingdom, Email: H.Sadeghipouya@coventry.ac.uk

Eshmaiel Ganjian

Professor, Centre for the Build and Natural Environment, Engineering, Environment, & Computing Building, Coventry University,
Coventry, CV1 2JH, United Kingdom, Email: e.ganjian@coventry.ac.uk

Adegoke Omotayo Olubanwo

Senior Lecturer, School of Energy, Construction and Environment, Sir John Laing Building, Coventry University, Coventry, CV1 2HF,
United Kingdom, Email: aa7878@coventry.ac.uk

Morteza Khorami

Lecturer, School of Energy, Construction and Environment, Sir John Laing Building, Coventry University, Coventry, CV1 2HF, United
Kingdom, Email: aa8186@coventry.ac.uk

Abstract

The commonly accepted Cathodic Protection (CP) criterion i.e. 100mV decay evolves from experimental investigations and may not always be accurate. Alternatively, corrosion rate monitoring can assess the adequacy of CP. This work examines the possibility of predicting the corrosion rate of steel in concrete using polarization data induced by known applied current density using Butler Volmer equation. For this, the value of cathodic Tafel slope (β_c) plays an important role; decreasing β_c from 210 to 60mV, decreases the corrosion rate by 92% at 20mA/m² current density.

* Corresponding author

26 The adequacy of the proposed method is evaluated by applying Impressed Current Cathodic
27 Protection (ICCP) to concrete specimens which have a zinc rich paint (ZRP) as an external
28 anode for a short duration of time. Results showed that to achieve at least 100mV of
29 depolarization, the applied current density should be at least 7 times the corrosion rate for the
30 ZRP anode. However, this holds true, considering the short duration of the tests. Prediction of
31 the corrosion rate of steel from potential shift forms the basis for the improved CP
32 performance criterion for reinforced concrete structures.

33 **Keywords:** Corrosion; Reinforced Concrete; Cathodic Protection; Potential Shift; Butler
34 Volmer Equation, Corrosion Rate

35 1. Introduction

36 Cathodic protection (CP) is an electrochemical technique used for halting or reducing the rate
37 of corrosion in reinforced concrete structures without having to remove chloride-
38 contaminated concrete [1–6]. In 1982, the U.S. Federal Highway Administration
39 memorandum stated that ‘the only rehabilitation technique that has been proven to stop
40 corrosion in salt-contaminated bridge decks regardless of the chloride content of the concrete
41 is cathodic protection’[7]. It is cost effective in the long run compared to other
42 electrochemical techniques. It can treat a larger area simultaneously and most importantly
43 does not give rise to incipient anode problems. Therefore, it is the most suited repair
44 technique to be employed in chloride contaminated structures [8].

45 The principle of CP is to deliver an appropriate cathodic polarization current to the protected
46 structure so that the potential of the protected structure is negatively shifted such that the
47 corrosion rate is either reduced or the steel reaches its passivation [2,9]. The suitability of CP
48 can be assessed on two bases: 1) it involves thermodynamic considerations which include
49 moving steel potential to the immune zone of Pourbaix diagram, 2) It involves examining the

50 kinetics of the involved reactions based on experimental measurements of current to potential
51 relationships of both cathodic reactions and metal dissolutions [10]. Some of the methods
52 used for monitoring are: Absolute Potential, Polarization curves, Depolarization method and
53 AC impedance response. The most commonly used method for CP monitoring for
54 atmospherically exposed structures is based on BS EN ISO 12696 criteria i.e. a)
55 Instantaneous OFF potential more negative than -720 mV vs Ag/AgCl/0.5MKCl (silver-silver
56 chloride) or b) 100 mV decay criterion [11]. However, the adequacy of 100 mV criterion has
57 been challenged by some researchers and the theoretical basis for its use is still subject to
58 investigation [12]. Moreover, 100 mV decay measurement alone might not be enough to
59 accurately predict corrosion state of rebar. Therefore, for more accurate determination of
60 corrosion state and to assess future corrosion risk, it is necessary to determine the corrosion
61 rate of steel in concrete.

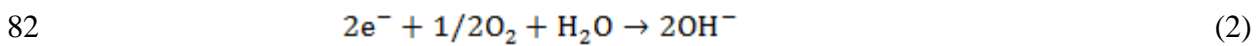
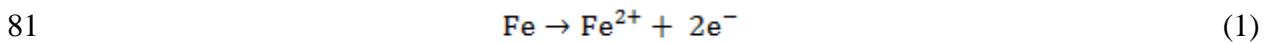
62 Corrosion rates are related to potential shifts and applied current density [13]. Stern and
63 Geary, developed an experimental procedure for measuring corrosion rates known as Linear
64 Polarization Resistance technique (LPR) [14]. The LPR method provides quantitative
65 information on corrosion rates; however, the value obtained is an instantaneous value and is
66 largely influenced by climatic changes such as temperature and humidity [15,16]. In this
67 paper, an alternative approach is suggested to monitor the corrosion rate of steel in concrete
68 after the application of cathodic protection, using the polarization data.

69 This work examines the adequacy of cathodic protection through the Butler Volmer equation
70 and tests its validity when applied to reinforced concrete. The adequacy is tested by applying
71 Impressed Current Cathodic Protection (ICCP) to concrete specimens having Zinc Rich Paint
72 (ZRP) as an anode system. Zinc-rich paints (ZRPs) are efficiently used as an anticorrosion

73 paint on ferrous metals and as a substitute to hot-dip galvanizing [17]. They are used as a
74 conductive coating anode for ICCP system in the present study.

75 2. Theoretical Basis

76 Considering equilibrium at any given point on the metal surface, the rate of forward and
77 backward reactions is equal. In concrete, at equilibrium conditions, reactions given by Eq. 1
78 and 2 are equal at steel surface. However, when cathodic and anodic half cells are ionically
79 (through concrete pore solution) and metallicity (through reinforcement) connected, a net
80 current flows between them and equilibrium potential shifts through polarization [18].



83 If the concentrations of the reactants and products at the electrode surface are the same as in
84 the bulk solution, the difference in potential from the reversible potential for a given reaction
85 is called activation overvoltage or charge transfer overvoltage [19]. For such reactions, the
86 relationship between the rate of reaction, which can be expressed by a current density i , and
87 the driving force for the reaction, or potential E , is given by the Butler-Volmer equation (Eq.
88 3) [19,20]:

$$89 \quad i = i_c - i_a = i^o \left\{ \exp\left(\frac{-\alpha_c F \eta}{RT}\right) - \exp\left(\frac{\alpha_a F \eta}{RT}\right) \right\} \quad (3)$$

90 Where $\eta = E - e_e$ i.e. the difference between the potential, E , when a net current flows through
91 electrochemical cell and reversible half-cell potential, e_e ; i^o (A/m^2) is exchange current
92 density; R is Gas Constant; F is Faraday's Constant; T is Absolute Temperature and α_c is the

93 fraction of total energy that decreases the energy barrier for cathodic reactions and α_a is the
 94 fraction of total energy that increases the energy barrier for anodic reactions.

95 At large over potential (η) and anodic partial current, the cathodic term becomes negligible
 96 and above equation is simplified to:

$$97 \quad i = -i_a = i_c \quad (4)$$

$$98 \quad i_a = i^0 \exp\left(\frac{-\alpha_a F \eta}{RT}\right) \quad (5)$$

99 Anodic sites on a steel surface are mainly polarized through the activation polarization [18].
 100 Rearranging the above equation gives,

$$101 \quad \eta_a = E_a - E_{Fe} = \beta_a \log \frac{i_a}{i^0} \quad (6)$$

102 Where, E_a (V) is polarized anodic potential, E_{Fe} is as given in Eq. 7, β_a (V/dec) is anode Tafel
 103 slope given by $\beta_a = (2.3RT/\alpha_a F)$, i^0 (A/m²) is anodic exchange current density and i_a (A/m²) is
 104 anodic current density.

$$105 \quad E_{Fe} = 0.440 - 0.0295 \log [Fe]^{2+} \quad (7)$$

106 On the other hand, cathodic sites on a steel surface can be polarized through both activation
 107 and concentration polarization, given by:

$$108 \quad \eta_c = E_c - E_{O_2} = \beta_c \log \frac{i_c}{i^0} - \frac{2.303RT}{nF} \log \left(\frac{i_L}{i_L - i_c} \right) \quad (8)$$



110 Where, E_c (V) is polarized cathodic potential, E_{O_2} as given in Eq. 9, β_c (V/dec) is cathode
 111 Tafel slope given by $\beta_c = (-2.3RT/\alpha_c F)$, i^o (A/m²) is cathodic exchange current density, i_c
 112 (A/m²) is cathodic current density, n is no. of electrons and i_L is limiting current density (Eq.
 113 10):

$$114 \quad E_{O_2} = 1.229 + 0.0148 \log[O_2] - 0.0591 pH \quad (9)$$

$$115 \quad i_L = \frac{DnFC_{O_2}}{d} \quad (10)$$

116 Where d (m) is diffusion layer thickness, D (m²/s) is oxygen diffusion coefficient, C_{O_2}
 117 (mol/m³ pore solution) is the concentration of dissolved oxygen on the concrete surface. The
 118 concentration polarization occurs only when oxygen availability at the cathodic site is not
 119 enough to sustain the oxygen reduction process [18].

120 In the 1950s, the Butler Volmer equation was simplified by assuming that the potential shift
 121 was small (10-20 mV). The relationship between current and potential was approximated to
 122 be linear rather than exponential when measured close to equilibrium potential and the linear
 123 polarization method was developed. Thus, approximating the exponential terms of the above
 124 B-V equation (Equation 3) based on ($e^x = 1 + x$):

$$125 \quad \exp\left(\frac{-\alpha_n F \eta}{RT}\right) = 1 + \left(\frac{-\alpha_n F \eta}{RT}\right) \quad \text{and} \quad \exp\left(\frac{(1-\alpha)_n F \eta}{RT}\right) = 1 + \left(\frac{(1-\alpha)_n F \eta}{RT}\right) \quad (11)$$

$$126 \quad i = -i^o \frac{nF\eta}{RT} = \frac{B}{Rp} \quad (12)$$

127 Where $R_p = (RT/nFi^0)$ is polarization resistance and B is Stern Geary constant. The value of
 128 Stern Geary Constant i.e. B ($B = \frac{\beta_a \beta_c}{2.303(\beta_a + \beta_c)}$) is typically used as 26 mV for an active steel
 129 and 52 mV for a passive steel [21,22]

130 The LPR method is most widely used to measure corrosion rates. However, the value
 131 obtained through LPR is approximated, instantaneous and largely influenced by climatic
 132 changes such as temperature and humidity [15,16]. This may lead to over or underestimation
 133 of corrosion rates. However, the LPR method cannot be used at potential shifts above 20mV,
 134 thus limiting its use for corrosion rate estimation for monitoring cathodic protection.

135 Alternatively, for Cathodic Protection, using the polarization data, corrosion rate can be
 136 predicted using the Butler Volmer Equation. Modifying equation 3 and substituting
 137 $\beta_c = (-2.3RT/\alpha_c F)$, $\beta_a = (2.3RT/\alpha_a F)$, $i = i_{app}$, $i^0 = i_{corr}$, $\eta = \Delta E$

$$138 \quad i = i^0 \left\{ \exp \left(\frac{2.3\eta}{\beta_c} \right) - \exp \left(\frac{-2.3\eta}{\beta_a} \right) \right\} \quad (13)$$

$$139 \quad i_{appl} = i_{corr} \left\{ \exp \left(\frac{2.3\Delta E}{\beta_c} \right) - \exp \left(\frac{-2.3\Delta E}{\beta_a} \right) \right\} \quad (14)$$

140 Where i_{appl} is the applied current density, i_{corr} is the corrosion rate, ΔE is the potential shift
 141 and β_a and β_c are constants. This will give a better and more accurate prediction of the
 142 corrosion rate in comparison to LPR.

143 In the present paper, this method is used to predict corrosion rate after cathodic protection of
 144 steel.

145 3. Experimental Method

146 3.1 Specimens

147 Three reinforced concrete slab specimens of size 200×200×70 mm were made of C32/40
148 grade concrete with a water-cement ratio of 0.5. The details of the concrete mix proportions
149 are presented in **Table 1**. Each specimen contained two 10 mm diameter ribbed steel bars
150 with an exposed length of 100 mm and a silver/ silver chloride (Ag/AgCl/0.5MKCl)
151 reference electrode. 3% NaCl solution was used for both curing and mixing to investigate the
152 performance of cathodic protection and its equivalent percentage by weight of cement was
153 deliberately added to the mixing water during casting. Specimens were demoulded after 24
154 hours and cured in potable water for a total period of 28 days.

Mix	w/c Ratio	Water (kg/m ³)	Ordinary Portland Cement (kg/m ³)	Sand (kg/m ³)	Gravel (kg/m ³)	Chloride (kg/m ³)
3% Chloride	0.5	180	360	640.5	1189.5	10.8

155 **Table 1. Mix proportioning of concrete specimens**

156 The surface of the specimens was prepared by wire brushing so that it attains medium
157 roughness. Then primary anode conductor (Anomet Cu/Nb/Pt wire of 2mm diameter) was
158 fixed on the top surface of concrete slab using epoxy resin. Then, the top face of each slab
159 specimen was painted with three layers of Zinc Rich Paint (ZRP), making sure that the
160 primary anode conductor is covered with the ZRP (**Fig. 1**) [23]. ZRP was used as an anode
161 material to provide an impressed current cathodic protection to steel in concrete. Because of
162 the pending patent and commercial confidentiality, it is not possible to disclose the full
163 chemical composition of the ZRP. The specimens were then kept in the curing tank
164 containing 3% NaCl water so that the samples were partially submerged in the salt solution.
165 The environmental temperature conditions were kept constant at 23±1°C.



166 **Fig. 1. Concrete specimen with Zinc Rich Paint (ZRP) primary anode**

167 **3.2 Measurement**

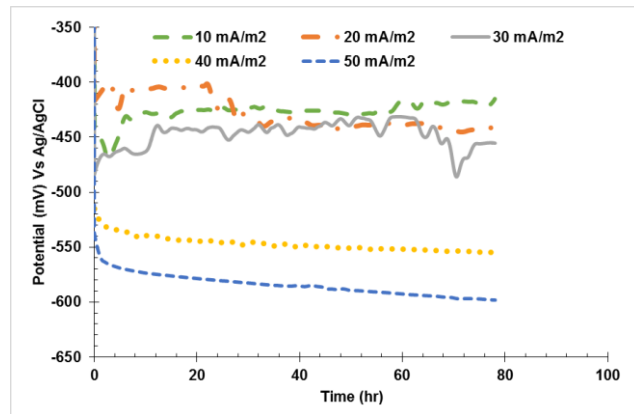
168 The cathodic polarization test was carried out on the specimens at five levels of current
169 densities, i.e., 10, 20, 30, 40 and 50 mA/m² of steel surface area, which were approximately
170 3.12, 6.25, 9.37, 12.5 and 15.62 mA/m² of the anode surface area. Each sample was polarized
171 five times for different level of current densities. The constant current output was supplied for
172 3 days at each current level as steel/concrete potential shift became negligible after 3 days,
173 and the polarization characteristics were recorded every minute using a computerized data
174 logger. After 3 days, the ICCP system was switched off and instant-off potentials were
175 recorded. The depolarization was continuously monitored using the computerized data
176 logging for a 24-hour period, at a 1-minute interval. The polarization and depolarization data
177 obtained from the application of various current densities in the experiment mentioned above
178 were used to assess the corrosion rate using the Butler Volmer equation (Eq. 14).

179 The LPR test was performed to determine the initial corrosion rate of the specimen before the
180 application of CP by applying a small perturbation using a Potentiostat (make: Digi-Ivy,
181 model DY 2300) to the slab specimens. In this method, reinforcements were polarized at a
182 sweep rate of 0.01V/min within the range of potential change from -20 mV to +20 mV.

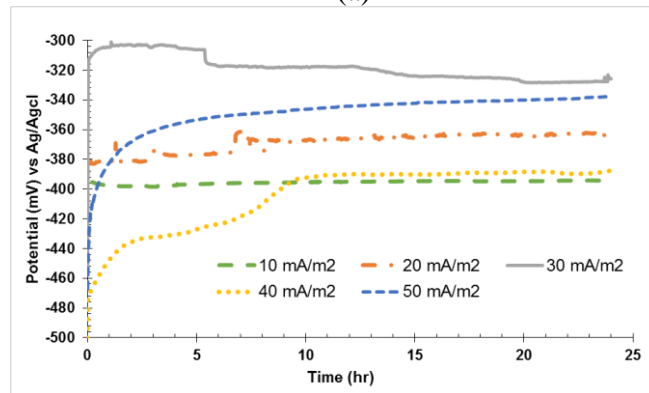
183 **4. Experimental Results and Discussion**

184 **4.1 Cathodic Polarization of Steel in Concrete using ZRP Anode**

185 The polarization and depolarization behavior evaluation of the ZRP anode with five different
186 current densities (10, 20, 30, 40 and 50 mA/m² per steel surface area) respectively are shown
187 in **Fig. 2**. Some spikes were observed in the graph due to the fluctuation in the power supply
188 to maintain a constant current.



(a)



(b)

189 **Fig. 2. (a) Polarization and (b) Depolarization behaviour of specimens at five different current**
190 **densities w.r.t Ag/AgCl/0.5MKCl reference electrode**

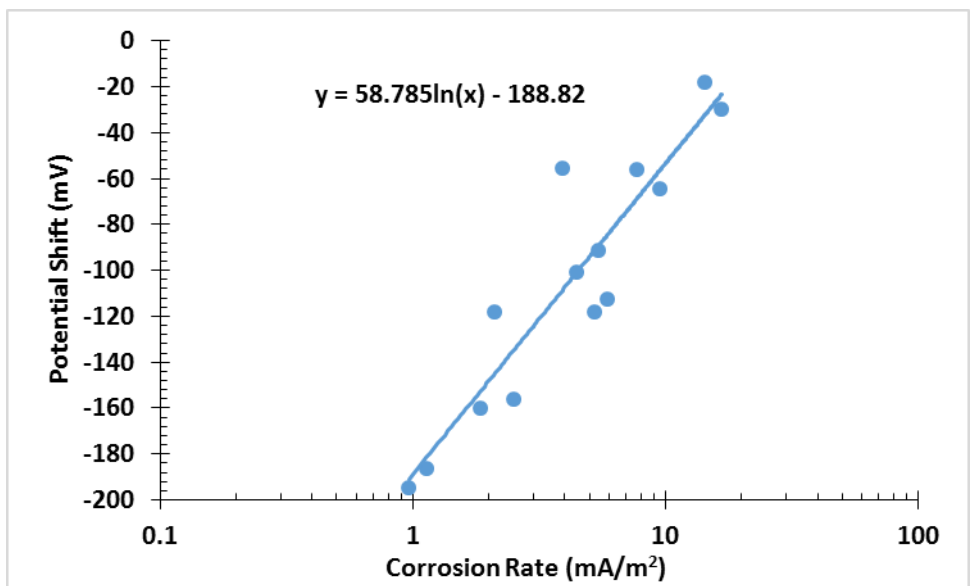
191 The steel/concrete potential shift and potential decay for each current density is shown in
192 **Table 2**. Potential shift is used to describe the difference between pre-energization potential
193 and instant off potential, whereas potential decay is used to describe the extent of
194 depolarization from instant off potentials. It can be observed that the higher the applied
195 current density, the higher the steel/concrete potential shift. Moreover, the 100 mV decay

196 criterion was met at 40 and 50 mA/m² of current density per steel surface area. The instant off
 197 potentials are IR free potentials.

Current density/ steel area (mA/m ²)	Current density/ anode area (mA/m ²)	Pre energization Potential (mV)	Instant Off Potential (mV)	Steel/Concrete Potential Shift (mV) vs Ag/AgCl/0.5MKCl	24 hr Decay (mV) vs Ag/AgCl/0.5MKCl
10	3.12	-393	-411	-18	16
20	6.25	-320	-376	-56	48
30	9.37	-318	-383	-65	80
40	12.50	-300	-486	-186	180
50	15.62	-342	-498	-156.0	153

198 **Table 2. Summary of polarization test results**

199 Further, corrosion rate was determined from the modified BV equation (Eq. 14) using the
 200 potential shift and the applied current density data and assuming an anodic and cathodic Tafel
 201 slope of 120 mV. The relationship between potential shift and corrosion rate is shown in **Fig.**
 202 **3.** The negative shift in steel/concrete/electrode corrosion potential is accompanied by a
 203 logarithmic decrease in the corrosion rate i.e. the higher the potential shift during
 204 polarization, the lesser the corrosion rate.



205 **Fig. 3. Relationship between potential shift and corrosion rate**

206 As per BS EN ISO 12696: 2016 [11], the boundary between steel in a passive state and low
 207 corrosion risk is at an average of 2 mA/m² corrosion rate. From **Fig. 3**, it can be seen that in
 208 order to move steel/concrete/electrode potential to the passive zone, a minimum of 150 mV
 209 potential shift is required during ICCP using a ZRP anode system. However, this criterion
 210 holds true only considering the short period of testing. For a longer period of polarization, the
 211 potential shift required might be different.

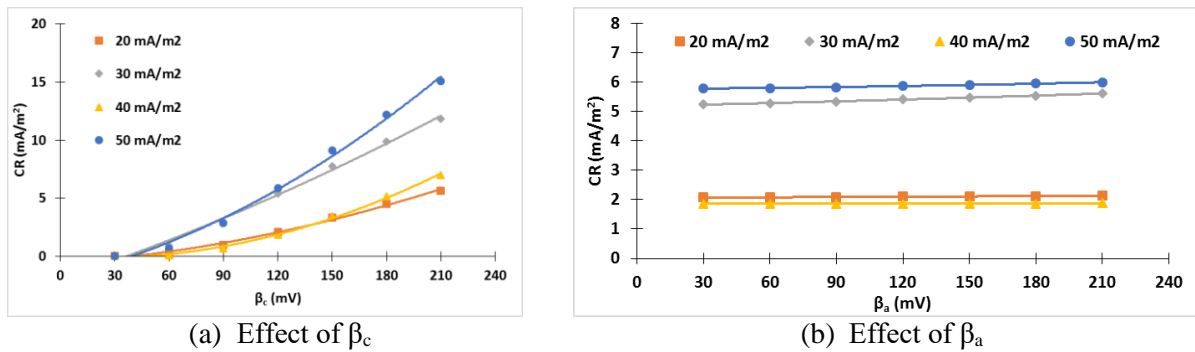
212 **Table 3** shows the corrosion rate measured using the LPR and BV methods before and after
 213 the polarization respectively. A decrease in corrosion rate is observed after the application of
 214 CP. Corrosion rate could not be determined from the LPR after polarization as it is limited for
 215 potential shifts less than 20 mV.

Applied Current Density (mA/m ²)	Corrosion Rate before CP: LPR (mA/m ²)	Corrosion Rate after CP: BV (mA/m ²)
10	19.1	18.0
20	19.6	14.0
30	11.7	10.6
40	16.5	1.2
50	9.4	3.9

216 **Table 3: Corrosion rate before and after polarization**

217 **4.2 Effect of Tafel slope on Corrosion Rate Estimation**

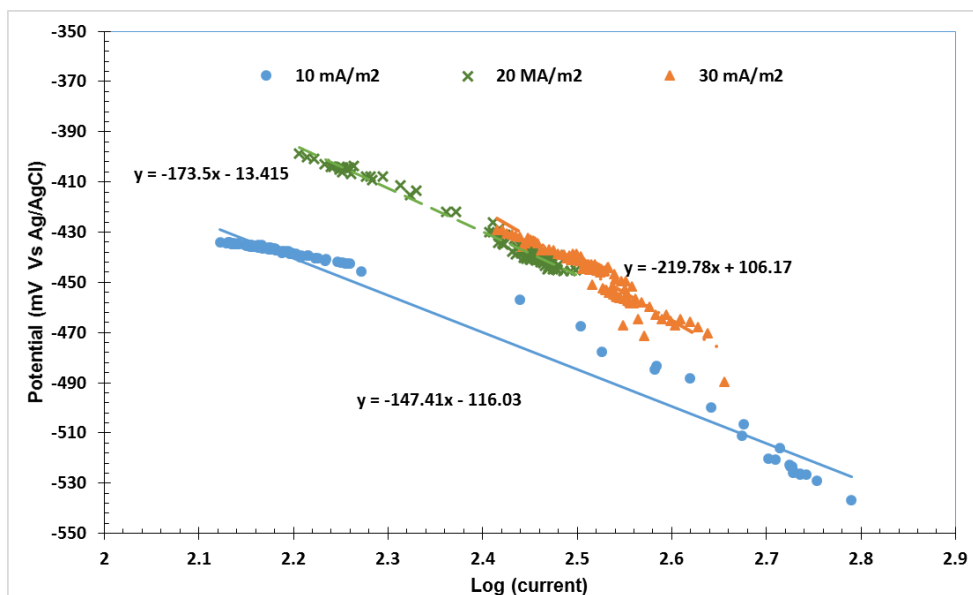
218 For on-site measurement, to predict the corrosion rate from linear polarization resistance
 219 method, $\beta_a = \beta_c = 120$ mV, which gives B=26 mV is recommended [16]. **Fig. 4.** shows the
 220 effect of cathodic and anodic Tafel slopes on the corrosion rate estimation at different current
 221 densities. The values are obtained by changing β_c and β_a value from 30 to 210 mV and using
 222 potential shift data from the polarization results.



223 **Fig. 4. Effect of (a) Cathodic and (b) Anodic Tafel slope on corrosion rate estimation at different**
 224 **current densities**

225 It can be observed that the effect of the anodic Tafel slope is small when compared to the
 226 cathodic Tafel slope. An increase of β_c value from 60 to 210 mV, increased the corrosion rate
 227 from 0.4 to 5.7 mA/m² at 20 mA/m² current density. On the other hand, a change in β_a from
 228 60 to 210 mV increased corrosion rate slightly from 2.07 to 2.13 mA/m² at 20 mA/m². Hence,
 229 corrosion rate estimation is more sensitive to the β_c value, and considering it as a constant
 230 value may result in errors in corrosion rate prediction.

231 Thus, for further analysis, β_c is predicted by plotting the change in steel/concrete/electrode
 232 potential against the logarithm of the applied current after each polarization. The slope of the
 233 curve will give an indication of the cathodic Tafel slope (**Fig. 5**).

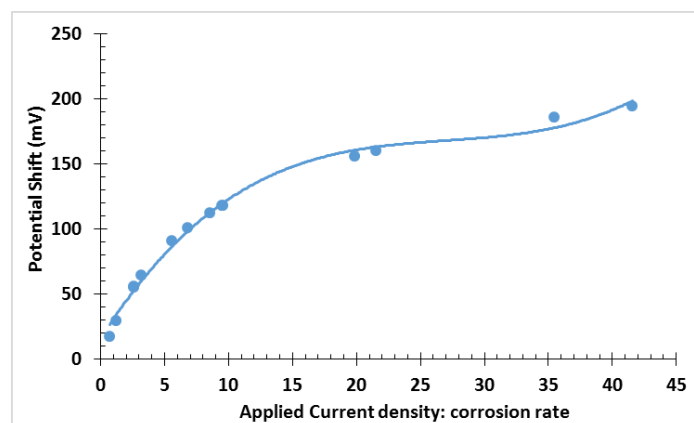


234 **Fig. 5. Prediction of cathodic Tafel slope from a potential-current graph**

235 The tafel slopes obtained were 147 mV, 173 mv and 219 mV for 10, 20 and 30 mA/m² of
236 current density respectively. In all the cases, the estimated cathodic Tafel slope is more than
237 120 mV. Thus a Tafel slope of 120 mV used to evaluate the protection level will result in
238 underestimation of the corrosion rate. This will risk suggesting a low corrosion that may not
239 be the case in practice.

240 4.4 Protection Criteria

241 The steel/concrete potential shift vs Ag/AgCl/0.5MKCl is plotted against the ratio of the
242 applied current density to corrosion rate from Butler Volmer (calculated from Eq. 14) in **Fig.**
243 **6**. It can be observed that a higher ratio of applied current density to corrosion rate is
244 accompanied by a higher potential shift.



245 **Fig. 6. Relationship between potential shift and the ratio of the applied current density to**
246 **corrosion rate calculated from polarization data**

247 As mentioned above, the most commonly used and recommended cathodic protection
248 monitoring criterion is to measure 100 mV potential decay following the interruption of the
249 polarization current [11,24]. This implies that in order to achieve this criterion, at least 100
250 mV of potential shift is required. Thus, from **Fig. 6**, it can be estimated that when the ZRP is
251 used as the primary anode for cathodic protection of steel in concrete, to achieve this
252 criterion, the applied current density should be at least 7 times the corrosion rate. This was in
253 close agreement with the ratio suggested by Glass et al. [12]. As in all the specimens, steel
254 was in a highly chloride contaminated environment before application of ICCP, thus the steel

255 was in a moderate to high corrosion risk state. Considering the boundary between moderate
256 and high corrosion risk, as recommended by the Concrete Society Technical Report No. 60
257 [25] to be average 5 mA/m^2 corrosion rate, the required current density to satisfy ICCP
258 protection criterion is minimum 7 times the corrosion rate i.e. 35 mA/m^2 per steel surface
259 area.

260 This confirmed the previous postulate where 40 mA/m^2 per steel surface area equivalent to
261 12.5 mA/m^2 per anode surface area was obtained as an optimum current density required for
262 cathodic polarization of steel in concrete using ZRP anode to satisfy 100 mV decay criterion.

263 Moreover, it was observed in **Fig. 3** that to move steel/concrete potential to a passive zone in
264 the case of using the ZRP anode system for cathodic protection, at least 150 mV potential
265 shift is required. Thus from **Fig. 6**, it is estimated that the applied current density should be at
266 least 15 times the corrosion rate to achieve 150 mV potential shift. Since the optimum applied
267 current density is 40 mA/m^2 per steel surface area (i.e. 12.5 mA/m^2 per anode surface area), the
268 achievement of this implies that steel is in near passive state.

269 However, this postulate holds true considering the short duration of the test, as a result BS
270 EN ISO 12696 criteria (a) [11] was not achieved for lower applied current densities. Hence a
271 higher current density was applied. Moreover, samples were polarized in partially saturated
272 conditions, thus requiring a higher potential shift to satisfy the BS EN ISO 12696 criterion (b)
273 [11]. For atmospherically exposed concrete specimens polarized for longer durations,
274 criterion (b) could be met with a smaller current density.

275 **5. Conclusion**

276 Potential shift data obtained from polarization results by applying a known current density
277 may be used to successfully estimate the corrosion rate of steel in concrete using the Butler
278 Volmer equation.

279 Moreover, it was observed that the cathodic Tafel slope (β_c) plays an important role in
280 corrosion rate estimation. Keeping this value constant, as in the case of LPR, results in an
281 underestimation of corrosion rate. Moreover, results showed that to achieve at least 100 mV
282 of depolarization, the applied current density should be at least 7 times the corrosion rate,
283 which is true considering the short duration of the test. For atmospherically exposed concrete
284 that is polarized for a longer period of time, CP performance criteria could be achieved for
285 lower current density. Hence, predicting corrosion rates from the BV equation using potential
286 shift forms the basis for an improved cathodic protection performance criterion for
287 atmospherically exposed reinforced concrete.

288 6. References

- 289 [1] R.B. Polder, W.H.A. Peelen, B.T.J. Stoop, E.A.C. Neeft, Early stage beneficial effects
290 of cathodic protection in concrete structures, *Mater. Corros.* 62 (2011) 105–110.
291 doi:10.1002/maco.201005803.
- 292 [2] J. Xu, W. Yao, Current distribution in reinforced concrete cathodic protection system
293 with conductive mortar overlay anode, *Constr. Build. Mater.* 23 (2009) 2220–2226.
294 doi:10.1016/j.conbuildmat.2008.12.002.
- 295 [3] A. Byrne, N. Holmes, B. Norton, State-of-the-art review of cathodic protection for
296 reinforced concrete structures, *Mag. Concr. Res.* 68 (2016) 1–14.
297 doi:10.1680/jmacr.15.00083.
- 298 [4] P. Pedferri, Cathodic protection and cathodic prevention, *Constr. Build. Mater.* 10
299 (1996) 391–402. doi:10.1016/0950-0618(95)00017-8.
- 300 [5] L. Bertolini, F. Bolzoni, M. Gastaldi, T. Pastore, P. Pedferri, E. Redaelli, Effects of
301 cathodic prevention on the chloride threshold for steel corrosion in concrete,
302 *Electrochim. Acta.* 54 (2009) 1452–1463. doi:10.1016/j.electacta.2008.09.033.
- 303 [6] J. Bennett, J.B. Bushman, J. Costa, P. Noyce, Field Application of Performance
304 Enhancing Chemicals to Metallized Zinc Anodes, *Corrosion*. paper no. (2000) Paper

- 305 No.00031. <http://www.onepetro.org/mslib/servlet/onepetropreview?id=NACE-00629>.
- 306 [7] US Federal Highway Administration, Long-term effectiveness of cathodic protection
307 systems on highway structures, Publ. No. FHWA-RD-01-096, FHWA. (2001).
308 <http://scholar.google.com/scholar?hl=en&btnG=Search&q=intitle:Long->
309 [Term+Effectiveness+of+Cathodic+Protection+Systems+on+Highway+Structures#0](http://scholar.google.com/scholar?hl=en&btnG=Search&q=intitle:Long-Term+Effectiveness+of+Cathodic+Protection+Systems+on+Highway+Structures#0).
- 310 [8] J. Broomfield, Anode Selection for Protection of Reinforced Concrete Structures,
311 *Mater. Perform.* 46 (2007).
- 312 [9] P. Marcassoli, A. Bonetti, L. Lazzari, M. Ormellese, Modeling of potential distribution
313 of subsea pipeline under cathodic protection by finite element method, *Mater. Corros.*
314 *Und Korrosion.* 66 (2015) 619–626. doi:10.1002/maco.201407738.
- 315 [10] P. Chess, Gronvold, Karnov, Cathodic protection of steel in concrete, 1998.
316 <http://medcontent.metapress.com/index/A65RM03P4874243N.pdf>.
- 317 [11] British Standard Institution, Cathodic protection of steel in concrete, BS EN ISO
318 12696: 2016, London 2016.
- 319 [12] G.K. Glass, A.M. Hassanein, N.R. Buenfeld, Monitoring the Passivation of Steel in
320 Concrete Induced By Cathodic Protection, *Corros. Sci.* 39 (1997) 1451–1458.
321 doi:10.1016/S0010-938X(97)00051-6.
- 322 [13] G.K. Glass, a. C. Roberts, N. Davison, Hybrid corrosion protection of chloride-
323 contaminated concrete, *Proc. ICE - Constr. Mater.* 161 (2008) 163–172.
324 doi:10.1680/coma.2008.161.4.163.
- 325 [14] M. Stern, A.L. Geary, Electrochemical Polarization I. A Theoretical Analysis of the
326 Shape of Polarization Curves, *J. Electrochem. Soc.* 104 (1957) 559.
327 doi:10.1149/1.2428653.
- 328 [15] B. Elsener, Corrosion rate of steel in concrete-Measurements beyond the Tafel law,
329 *Corros. Sci.* 47 (2005) 3019–3033. doi:10.1016/j.corsci.2005.06.021.
- 330 [16] C. Andrade, C. Alonso, Test methods for on-site corrosion rate measurement of steel
331 reinforcement in concrete by means of the polarization resistance method, *Mater.*

- 332 Struct. 37 (2004) 623–643. doi:10.1007/BF02483292.
- 333 [17] N. Hammouda, H. Chadli, G. Guillemot, K. Belmokre, The Corrosion Protection
334 Behaviour of Zinc Rich Epoxy Paint in 3% NaCl Solution, *Adv. Chem. Eng. Sci.* 1
335 (2011) 51–60. doi:10.4236/aces.2011.12009.
- 336 [18] A. Poursaeed, *Corrosion of Steel in Concrete Structures*, 1st ed., Elsevier Science,
337 London, 2016, 249-268. doi:10.1016/B978-1-78242-381-2.00001-8.
- 338 [19] G.S. Frankel, *Fundamentals of Corrosion Kinetics*, in: *Act. Prot. Coatings*, 2016: pp.
339 17–32. doi:10.1007/978-94-017-7540-3.
- 340 [20] Popov, *Corrosion Engineering: Principles and Solved Problems*, 1st ed., Elsevier,
341 Oxford, 2015. doi:10.2307/23499350.
- 342 [21] H. Song, V. Saraswathy, *Corrosion Monitoring of Reinforced Concrete Structures - A*
343 *Review*, *Int. J. Electrochem. Sci.* 2 (2007) 1–28.
- 344 [22] J.H. Bungey, S.G. Millard, G. Grantham, *Testing of Concrete in Structures*, Taylor and
345 Francis, Oxon: 1982.
- 346 [23] S.C. Das, H.S. Pouya, E. Ganjian, Zinc-Rich Paint As Anode for Cathodic Protection
347 of Steel in Concrete, *J. Mater. Civ. Eng.* 27 (2015) 1–9. doi:10.1061/(ASCE)MT.1943-
348 5533.0001243.
- 349 [24] NACE, *Impressed Current Cathodic Protection of Reinforcing Steel in*
350 *Atmospherically Exposed Concrete Structures*, NACE Int. SP0290 (2007).
- 351 [25] Concrete Society Technical Report, *Electrochemical tests for reinforcement corrosion*,
352 The Concrete Society 60, 2004.

353 **Declaration of Interest**

354 We wish to confirm that there are no known conflicts of interest associated with this
355 publication and there has been no significant financial support for this work that could have
356 influenced its outcome.